Local Dynamics of Stereoregular PMMAs Using Molecular Simulation

A. Soldera*

CEA-LR, BP 16, 37260 Monts, France

Y. Grohens

Laboratoire de Biologie et Chimie Moléculaire, Centre de Recherche, rue Saint-Maudé, 56325 Lorient Cedex, France

Received July 31, 2001; Revised Manuscript Received November 1, 2001

ABSTRACT: The physical origin of the large differences between the glass transition temperatures (T_g) exhibited by various stereoregular PMMA is not yet fully understood. Currently available theories on the glass transition phenomena are not able to predict the observed behavior. In this paper, results obtained from molecular dynamics (MD) simulations are presented. Actually, MD is a very powerful tool to investigate and differentiate the local dynamics of molecular groups embedded in either the backbone or the side chain. From the calculated WLF parameters it is found that the dynamics of the backbone is independent of the PMMA tacticity whereas the dynamics of the side chain strongly depends on the PMMA stereoregularity. However, since the frequency of side-chain rotations is more important in isotactic PMMA compared to syndiotactic, the overall mobility of the isotactic chains becomes higher. Consequently, according to the free volume concept, the T_g of isotactic PMMA is lower than the T_g of the syndiotactic isomer.

Introduction

Local molecular motions constitute the basic process of mechanical and physical phenomena. Among these events, the glass transition is of particular interest in polymer applications since it splits apart two domains of different use, namely, the glassy and the rubbery states. The study of the relationship between the local dynamics occurring during the glass transition and the chemical structure of polymers offers a specific regard. From an experimental viewpoint, spectroscopy techniques are particularly adapted to give insight into local motion during such a transition by investigating the nature of the relaxation processes. However, to highlight specific local motions, some difficulties could appear. In fact, one particular motion could not be easily retrieved since it is often combined with other motions. To compensate such limitations of experimental techniques, molecular modeling is perfectly suited.

In our investigation of the glass transition phenomona, poly(methyl methacrylate), PMMA, offers a particular benefit since according to its chain tacticity, a different glass transition temperature, T_g, is exhibited. The bulk T_g is generally ranging from 40 to 130 °C from isotactic to syndiotactic PMMA. Efforts have been made in the past to apply theoretical concepts to explain such a difference. Gibbs and DiMarzio (GD) promulgated the idea that the conformational energy ϵ (difference in energies between trans and gauche conformations) is the primary factor in determining the T_g of a polymer.[1] Experimentally[2] or by conformational energy calculations,[3] several workers clearly showed that significant differences in the conformational energy exist between the two isomers. Moreover, for the isotactic isomer, the side-chain conformation is found to differ as much in energy as do the backbone conformations. From a molecular simulation viewpoint, it has been shown in a previous paper[4] that intra- and intermolecular energies both contribute to the difference in the T_g's between the two PMMA configurations. The former energy takes into account connectivity, flexibility, and cross-term contributions while the latter energy is concerned with the nonbonding interactions. The isotactic configuration was revealed to exhibit a lower intermolecular energy than the syndiotactic while for the intramolecular energy it was the opposite. This difference in the intermolecular energy shows that the interactions between s-PMMA chains are less favored than between i-PMMA ones. Actually, such a behavior agrees with the second important parameter in the GD theory, namely the hole formation energy. This energy corresponds to the interaction between pairs of nonbonded but proximate segments. It has been shown to depend on the PMMA tacticity.[3] Hence, the interactions and the packing of the side groups have been envisaged as an important factor in the determination of the T_g. A specific study on the difference in the intramolecular energy between the two isomers is the subject of another article.[5]

From a dynamics viewpoint, Allen et al.[6] calculated from neutron scattering and NMR relaxation studies the rotation barriers of the α-methyl, which is 32 and 23 kJ/mol for solid s- and i-PMMA, respectively. Besides, in light of the theory of Adam and Gibbs,[7] who proposed that an enhanced degree of cooperativity is required at T_g, several workers[8,9] suggested that a certain population of isotactic sequences relax in a cooperative fashion well below the T_g of a conventional PMMA. Moreover, using 2-D NMR spectroscopy, Kuebler et al.[9] demonstrated that the unusual main-chain mobility below T_g is coupled to the β-relaxation process in *at*-PMMA. However, even if a certain amount of isotactic triads is present in the atactic chains, no mention is made to the possible influence of the tacticity in the cooperativity of the relaxation process.

* Author for correspondence: e-mail Armand.Soldera@cea.fr. Address after April 1, 2002: Université de Sherbrooke, Faculté des Sciences, Département de Chimie, Sherbrooke, Québec, J1K 2R1, Canada. E-mail: Armand.Soldera@Courrier.usherb.ca.

10.1021/ma011370q CCC: $22.00
Published on Web 12/20/2001

The local dynamics of polypropylene chain with different tacticities has been recently looked at through molecular dynamics simulations.[10] However, the two chains approximately possess the same T_g. Nevertheless, dynamics properties extracted from simulation were found to accurately match experimental data.[11] The present article thus proposes to draw a parallel between the experimental observations on the local dynamics and relaxation studies deduced from molecular simulations for the two PMMA stereomers. Compared with energetic analysis results, further insights to the understanding of the difference in T_g's between the two stereomers are provided.

Simulation Description. All the simulations are performed using the periodic boundary conditions.[12] The polymer chains, with 100 repeat units, propagate into the periodic box according to the self-avoiding walk technique[13] with the long-range nonbonded interactions described by Theodorou and Suter.[14] The procedure is implemented in the MSI (presently Accelrys) Amorphous_Cell software. From an experimental viewpoint, the dilatometric technique is currently employed to determine the T_g: the specific volume is reported for different temperatures as the system is cooled; the intercept of the lines joining the points of the two phases, namely the vitreous and rubbery, yields the value of the T_g. Atomistic MD gives the opportunity to explore this kind of time-dependent properties, but these simulations are limited by current computing resources to times of order picoseconds. Simulation cooling rates are much higher (of order 10^{10} K s^{-1}) than what could be achieved in even the fastest quenching experiment, and hence MD simulations will not access the same spectrum of conformational fluctuations. Despite that, the results can be regarded as relative and comparative between different kinds of polymers or different polymer microstructures. Each specific volume data point of the dilatometric experiment is obtained through a relatively short MD (110 ps) while considering the accurate *pcff* force field. All the details of the procedure can be found in a previous article.[4] For this study, configurations at temperatures above T_g are extracted. MD simulations with a duration of 1 ns at the different temperatures are then carried out.

As shown in a previous article,[4] simulated dilatometry provided T_g's of 157 and 212 °C for the iso- and syndiotactic PMMA configurations, respectively. The difference in T_g's between the two configurations, 55 °C, was found consistent with the experimental one, 69 °C. Such a result clearly indicates the accuracy of the *pcff* force field and the validity of the procedure (chain propagation, MD simulations). It has to be pointed out that this force field has been used by Eichinger et al.[15] to compute solubility parameters and cohesive energies with an highly accuracy. Moreover, *pcff* derived from the *cff91* force field, which is considered to be among the best force fields in regard to the conformational energies.[16] Consequently, *pcff* is appropriate to consider intermolecular interactions and to get acquainted with the conformational transitions of the polymer chain, in the polymer melt phase.

Results and Discussion

Procedure of Data Treatment. To specifically study the link between the motions responsible for the local dynamics with molecular processes accountable for the glass transition, the evolution in temperature of the correlation time has to be investigated. Such a progress actually follows the Vogel−Fulcher−Tammann (VFT) equation:

$$\tau(T) = A \exp\left(\frac{B}{T - T_0}\right) \tag{1}$$

T_0 is the temperature at which the configurational entropy vanishes. B can be related to the apparent activation energy through the following relation: $\Delta H_{ap} = BR$, where R is the perfect gas constant.[17] Actually, it is not an activation energy since the equation clearly shows a non-Arrhenius behavior at temperature above T_g. A similar empirical expression, the Williams−Landel−Ferry (WLF), equation, can also be used:

$$\log\left(\frac{\tau(T)}{\tau(T_g)}\right) = -\frac{C_1^g(T - T_g)}{C_2^g + T - T_g} \tag{2}$$

Actually, the WLF equations can be deduced from the VFT equation, and vice versa, according to the following equation:

$$\log(\tau(T)) = \frac{C_1^g C_2^g}{T - T_\infty} - C_1^g + \log(\tau(T_g)) \tag{3}$$

where

$$T_\infty = T_g - C_2^g$$

From both VFT and WLF equations, an apparent activation energy can be deduced: $\Delta H_{ap} = \Delta H_{ap}^{VFT}$ from the VFT equation, and $\Delta H_{ap} = \Delta H_{ap}^{WLF}$, with $\Delta H_{ap}^{WLF} = 2.303RC_1^gC_2^g$, from the WLF relation.[17] As a matter of fact, the determination of the correlation time with temperature of a specific part of the chain provides information on its local motion.

Using molecular simulation, local dynamics of the entire chain or only a small part of it can therefore be investigated at different temperatures. The acquisition of the correlation time associated with a bond vector at a specific temperature is achieved through the computation of the autocorrelation function. This function actually gives insights into the local dynamics. However, since one is interested in the decrease in time of the bond vector orientation, the second term of the Legendre polynomial is computed:

$$P_2(t) = \frac{3\langle(\mathbf{u}(t)\cdot\mathbf{u}(0))^2\rangle - 1}{2} \tag{4}$$

$\langle\mathbf{u}(t)\cdot\mathbf{u}(0)\rangle$ corresponds to the normalized autocorrelation function of the vector $\mathbf{u}$, with the brackets indicating that the average was performed on all the bond vectors, $\mathbf{u}$, along the chain. Examples of the evolution of the orientation function vs time of the C−H bond vector located on the isotactic backbone at different temperatures are displayed in Figure 1. The behavior of the orientation function is in agreement with experiment since at high temperatures, the decrease in the vector orientation is more rapid, meaning that the chain segments are more mobile.

Such a decorrelation is actually expressed by the correlation time. To get acquainted with this correlation time, the integration over all the time domain, theoretically from 0 to infinity, of the orientation function has

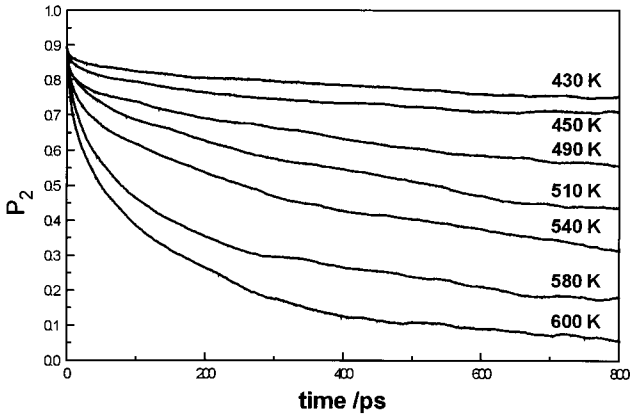

Figure 1. Decorrelation of the C−H bond vector located on the i-PMMA backbone at various temperatures.

to be carried out. The chosen way to compute it is to use a mathematical function which fits the $P_2(t)$ function.[18] Since the motion of the bond vector is not isotrope, the decorrelation cannot be fitted with a simple exponential function. To better describe it, a stretching exponential function, the Kolsrauch−Williams−Watt function, is employed:

$$\phi(t) = \exp\left[-\left(\frac{t}{\tau}\right)^{\beta}\right] \tag{5}$$

τ is a parameter often interpreted as the average relaxation time, and β represents the departure from a simple exponential decay: $0 < \beta < 1$. Actually, this function does not fit the $P_2(t)$ function at short times where librational motions occur but adequately expresses it for longer times where transitions between rotameric states take place. To consider short-time behavior, an exponential decay function can be added to the stretching exponential.[19] However, in our simulation to obtain τ and β, the procedure described by Antoniadis et al. is carried out,[18] and the fitting begins when the linearity in the graph of $\ln[-\ln(P_2)]$ vs $\ln(t)$ is reached. As a matter of fact, the adjustable parameters, τ and β, are found to more appropriately fit the longer times. The integration from 0 to infinity of the orientation function can then be carried out and gives the following form for the correlation time:

$$\tau_c = \frac{\tau}{\beta}\Gamma\left(\frac{1}{\beta}\right) \tag{6}$$

The correlation time, τ_c, at a specific temperature stemmed from the fitting parameters τ and β. The procedure is conducted at different temperatures for both PMMA tacticities and for two bond vectors: the C−H bond vector located on the CH_2 and the C═O bond vector. The behavior of the C−H bond vector reveals the transitions in the backbone motions, and it can be compared to experimental data, while the study of the C═O bond vector response unveils the side-chain behavior. It has to be pointed out that no experimental data on PMMA were found in the literature for the reorientation of the C═O bond vector with temperature.

WLF and VFT functions are then used to relate all the correlation times for both configurations and for both vectors. To access the C_1^g and C_2^g parameters, the procedure described by Dekmezian has been used:[20] $(T - T_g)$ is reported vs $-(T - T_g)\}/\log(\tau_c/\tau_g)$, with $\tau_g =$ 100 ps.

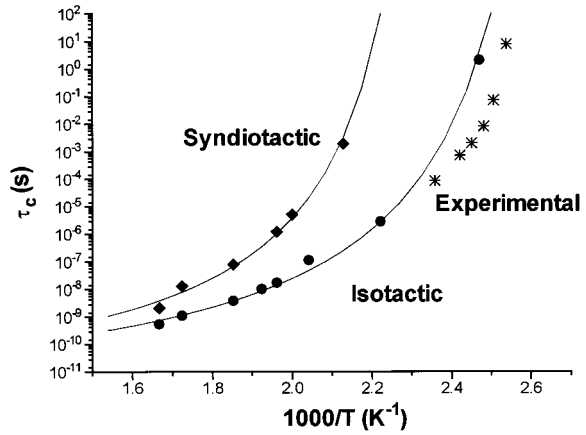

Figure 2. Correlation times of experimental *at*-PMMA (*), and of the i-PMMA (●) and s-PMMA (◆) C−H bond vector orientation, with respect to the inverse temperature times 1000. Are also displayed the fitting by a WLF equation (—).

Table 1. Parameters of the WLF and VFT Equations, C_1^g, C_2^g, and the Apparent Activation Energies, Extracted from MD Simulations, Associated with the Orientation of the C−H Bond Vector Located on the Backbone of the Two PMMA Stereomers

tacticity	C_1^g	C_2^g (K)	ΔH_{ap}^{WLF} (kJ mol^{-1})	ΔH_{ap}^{VFT} (kJ mol^{-1})
syndiotactic	13	37.8	9.4	11.9
isotactic	13.2	37.4	9.5	12.8

Backbone Chain Investigation. The procedure to access the correlation time and the WLF and VFT parameters was first applied to the C−H bond vector, along the backbone. The data extracted from simulation, the C_1^g and C_2^g parameters, and the apparent activation energies computed from the WLF and VFT equations for the two PMMA chain tacticities are reported in Table 1. Figure 2 displays the computed correlation times and the fits ensuing from the WLF equation.

From the literature, different WLF parameters and interpretations were found for PMMA. From viscoelastic measurements,[21] the C_1^g and C_2^g parameters were revealed different according to the chain tacticity of PMMA: the apparent activation energy of the syndiotactic configuration was found higher than that of the isotactic configuration. However, a certain portion of the free volume is necessary to achieve chain mobility at the glass transition. This volume has been shown by Fuchs et al. to be independent of the chain tacticity.[22] Since C_1^g is inversely proportional to the free volume fraction according to the free volume theory of the glass transition,[23] this parameter has to be independent of the chain tacticity. Finally, from the VFT equation obtained from mechanical and dielectric relaxation spectrometry, Bartenev found an apparent activation energy lower for the syndiotactic configuration than for the isotactic one.[24]

The simulated C_1^g parameters, 13 and 13.6 from Table 1, are in accordance with published data: experimentally, C_1^g ranged from 8.9 to 20.[21,22] Moreover, both chain configurations exhibit similar values, in agreement with Fuchs results.[22] However, a difference with experimental data is found with the simulated C_2^g parameter. Simulated T_g's are found higher than the experimental ones. Consequently, from the mathematical form of the WLF equation, a higher T_g implies a lower C_2^g value to allow the correlation times to be

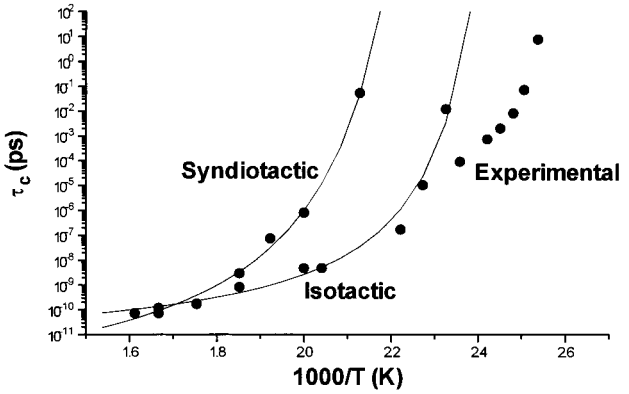

Figure 3. Correlation times of experimental *at*-PMMA (*), and of the i-PMMA (●) and s-PMMA (◆) C═O bond vector orientation, with respect to the inverse temperature times 1000. Are also displayed the fitting by a WLF equation (—).

Table 2. Parameters of the WLF and VFT Equations, C_1^g, C_2^g, and the Apparent Activation Energies, Extracted from MD Simulations, Associated with the Orientation of the C═O Bond Vector of the Two PMMA Stereomers

tacticity	C_1^g	C_2^g (K)	ΔH_{ap}^{WLF} (kJ mol^{-1})	ΔH_{ap}^{VFT} (kJ mol^{-1})
syndiotactic	15	36	10	11.5
isotactic	13	20	5	5

fitted. Nevertheless, qualitative interpretations can be deduced from the simulated data and can be compared with published results.

As shown in Table 1, both apparent activation energies, extracted from WLF and VFT fits, are in the same order and are comparable for both chain configurations. Consequently, the two chains of different tacticity present the same behavior at a specific temperature above T_g, i.e., at T_g + constant. However, at a given temperature, independent of the T_g, both chains exhibit different behaviors; the correlation times of the isotactic configuration are lower than those of the syndiotactic ones, in accordance with experimental data[25] (Figure 2). At a specific temperature the isotactic chains are therefore more mobile than the syndiotactic ones. The relaxation of the side chain has to be regarded to check the assumption of an influence of the local dynamics of the side group on the backbone. More specifically, the apparent activation energies associated with the C═O bond vector of both configurations are computed.

Side Chain Investigation. The procedure previously described for the computation of correlation times is applied to the C═O bond vector orientation. Figure 3 displays the computed correlation times and the WLF fit. The final results are summarized in Table 2.

The C_1^g parameters, 15 and 13 for s-PMMA and i-PMMA, respectively, are in the same range of experimental data for both configurations.[21,22] A lower value for i-PMMA is not significant to clearly debate on this result. The principal difference between the two configurations actually lies in the apparent activation energy. s-PMMA clearly exhibits a higher apparent activation energy than i-PMMA.

Actually, the computation of $P_2(t)$ related to the C═O bond vector includes three kinds of motion. The first motion, located in the short time region, corresponds to the librational motion: the vector does not move too much from the initial position; it stays in a potential well. It has to be pointed out that at low temperatures it is the main motion. On a larger time

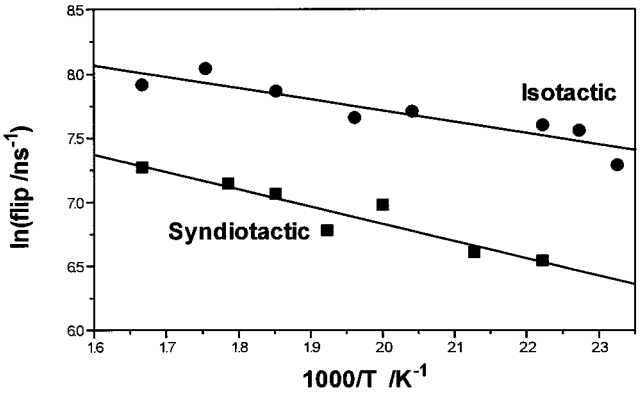

Figure 4. Neperian logarithm of the transition frequency of the side chain of i-PMMA (●) and s-PMMA (◆) with respect to the inverse temperature times 1000.

scale, the transitions between the *up* and *down* rotameric states of the side chain, defined by Sundararajan,[26] take place. Finally, rotations between rotameric states of the backbone occur. Actually, the boundaries between the associated times are not well-defined. Consequently, the difficulty arises to separate the different correlation times associated with these motions. As already pointed out, the librational motions do not intervene in the stretching exponential fitting of $P_2(t)$. The B values reported in Table 2 thus correspond to the rotations of the side chain and the backbone. Since they are clearly different for both stereomers, the transition frequency of the side chain between the two rotameric states, "up" and "down", i.e., the number of transitions by time unit, has to be computed in order to differentiate it from backbone motion. Figure 4 reports this frequency vs the inverse temperature.[27] Both configuration behaviors are clearly Arrhenius-like, as is expected for such a motion, which corresponds to a β relaxation. Consequently, an activation energy can be computed: 7.3 and 11.2 kJ/mol for i-PMMA and s-PMMA, respectively. It has to be noted that such an Arrhenius behavior was not detected in the simulated correlation time curves (Figure 3) since they include motions corresponding to both relaxing segments, backbone and side chain.

If some differences exist in the literature regarding the interpretation of VFT and WLF equations, publications on correlation times are more in accordance with each other. Spevacek et al. compared the correlation times of the two PMMA chain tacticities at temperatures above T_g:[25] the correlation times of the i-PMMA chains were found lower than that of the s-PMMA ones. Comparing the NMR data of poly(ethyl methacrylate), PEMA, and PMMA, Kuebler et al. showed that the side chain by its rotation implies a lower correlation time of the backbone.[9] The side chain rotation therefore seems directly related to the mobility of the backbone. To correlate this assumption, the study of a trajectory extracted from a MD simulation reveals changes in polymer chain conformation as a function of time. The occurrence of discrete jumps between rotameric states is thus clearly observed in Figure 5. In this figure, the variation of consecutive backbone and side chain dihedral angles of i-PMMA are displayed during a period of 100 ps extracted from a 500 ps simulation at 0 °C. At such a low temperature, both angles quite simultaneously change in the 0.1 ps time range, which corresponds to the interval between each data. It has to be pointed out that the dihedral angle changes shown in

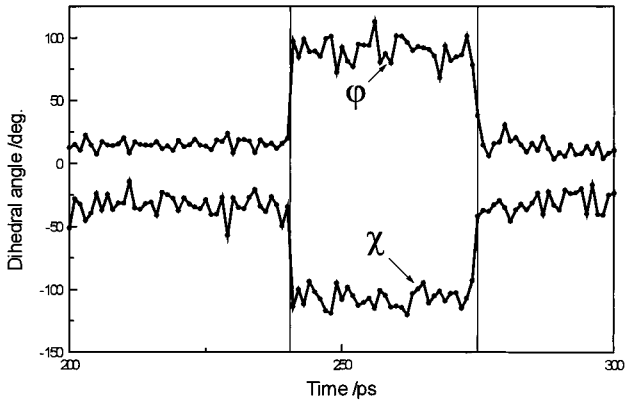

Figure 5. Variation of the dihedral angles of a backbone bond, φ, and its attached side chain bond, χ, with respect to time, for i-PMMA at 0 °C.

Figure 5 arise at a temperature lower than the T_g's. One can notice, at that temperature, the fast angle variation and the low time duration, 30 ps, of the bonds in the new rotameric states. The correlation between the dihedral angle motions of the side chain and the backbone is clearly observed in this figure. Studies are presently performed to quantify such a cooperativity and thus to observe the difference between the two stereomers.

A complex correlation involving concerted motions is likely to exist between the rotation of the PMMA side chain and the mobility of the backbone: the higher is the rotation frequency of the side chain, the higher is the mobility of the backbone. If the number of the side chain rotations increases, the number of backbone transitions between rotameric states also expands. Therefore, the backbone time correlation decreases, as could be observed from both experimental and simulation data. Consequently, the mobility of the backbone is extended. Finally, since the number of side chain rotations is more important in i-PMMA compared to s-PMMA at all temperatures, the overall mobility of i-PMMA becomes higher. Actually, such a behavior is in accordance with experimental T_g values since, according to the free volume theory, the greatest mobility of the polymer chains implies the lowest T_g.

Conclusion

In this paper, MD simulations are shown to be a powerful tool to investigate the T_g's of both PMMA stereomers. From the calculated apparent activation energy, the backbone mobility is not found to be tacticity dependent whereas the motion of the side chain is strongly influenced by the PMMA stereoregularity. Moreover, from experimental measurements the rotation of the side chain is shown to influence greatly the mobility of the backbone chain. Since the side chain in i-PMMA displays a higher frequency rotation than in s-PMMA, the mobility of the i-PMMA backbone chain is increased. Consequently, the T_g of i-PMMA is lower than the T_g of s-PMMA.

References and Notes

(1) Gibbs, J. H.; DiMarzio, S. F. *J. Chem. Phys.* **1958**, *28*, 373.
(2) O'Reilly, J. M.; Mosher, R. A. *Macromolecules* **1981**, *14*, 602−608.
(3) Vacatello, M.; Flory, P. J. *Macromolecules* **1986**, *19*, 405−415.
(4) Soldera, A. *Macromol. Symp.* **1998**, *133*, 21−32.
(5) Soldera, A., submitted to *Comput. Theor. Polym. Sci.*
(6) Allen, G.; Wright, C. J.; Higgins, J. S. *Polymer* **1974**, *15*, 319−325.
(7) Adam, G.; Gibbs, J. H. *J. Chem. Phys.* **1965**, *43*, 139−146.
(8) Sherif Faruque, H.; Lacabanne, C. *J. Mater. Sci.* **1990**, *25*, 321−324.
(9) Kuebler, S. C.; Schaefer, D. J.; Boeffel, C.; Pawalzik, U.; Spiess, H. W. *Macromolecules* **1997**, *30*, 6597−6609.
(10) Antoniadis, S. J.; Samara, C. T.; Theodorou, D. N. *Macromolecules* **1999**, *32*, 8635−8644.
(11) Smith, G. D.; Paul, W.; Monkenbusch, M.; Willner, L.; Richter, D.; Qiu, X. H.; Ediger, M. D. *Macromolecules* **1999**, *32*, 8857−8865.
(12) Allen, M. P.; Tildesley, D. J. *Computer Simulation of Liquids*; Clarendon Press: Oxford, 1987.
(13) Meirovitch, H. *J. Chem. Phys.* **1983**, *79*, 502−508.
(14) Theodorou, D. N.; Suter, U. W. *Macromolecules* **1985**, *18*, 1467−1478.
(15) Eichinger, B. E.; Rigby, D. R.; Muir, M. H. *Comput. Polym. Sci.* **1995**, *5*, 147−163.
(16) Petterson, I.; Liljetors, T. In *Reviews in Computational Chemistry*; Boyd, K. B. L. a. D. B., Ed.; VCH Publishers: New York, 1996; p 167.
(17) Ferry, J. D. *Viscoelastic Properties of Polymers*; John Wiley and Sons: New York, 1970; p 318.
(18) Antoniadis, S. J.; Samara, C. T.; Theodorou, D. N. *Macromolecules* **1998**, *31*, 7944−7952.
(19) Moe, N. E.; Ediger, M. D. *Macromolecules* **1995**, *28*, 2329−2338.
(20) Dekmezian, A.; Axelson, D. E.; Decheter, J. J.; Borah, B.; Mandelkern, L. *J. Polym. Sci., Polym. Phys. Ed.* **1985**, *23*, 367−385.
(21) Jasse, B.; Oultache, A. K.; Mounach, H.; Halary, J. L.; Monnerie, L. *J. Polym. Sci., Part B: Polym. Phys.* **1996**, *34*, 2007−2017.
(22) Fuchs, K.; Friedrich, C.; Weese, J. *Macromolecules* **1996**, *29*, 5893−5901.
(23) Sperling, L. H. *Introduction to Physical Polymer Science*; John Wiley and Sons: New York, 1992; p 340.
(24) Bartenev, G. M. *Vysokomol. Soedin.* **1999**, *41*, 936−944.
(25) Spevacek, J.; Schneider, B.; Straka, J. *Macromolecules* **1990**, *23*, 3042−3051.
(26) Sundararajan, P. R. *Macromolecules* **1986**, *19*, 415−421.
(27) Gee, R. H.; Boyd, R. H. *Comput. Theor. Polym. Sci.* **1998**, *8*, 91−98.

MA011370Q